

Reconciling the impact of mobile bottom-contact fishing on marine organic carbon sequestration

Pooran Khedri^{1,2}, Olivier Gourgue², Jochen Depestele³, Sandra Arndt^{1,4},
Sebastiaan J. van de Velde^{5,6,7,*}

¹Department of Geoscience, Environment and Society, Université libre de Bruxelles, 1050 Brussels, Belgium

²Operational Directorate Natural Environment, Institute of Natural Sciences, 1000 Brussels, Belgium

³Flanders Research Institute for Agriculture, Fisheries and Food (ILVO), 8400 Oostende, Belgium

⁴iC3, Center for Ice, Climate, Carbon and Cryosphere, UiT the Arctic University of Norway, 9019 Tromsø, Norway

⁵Department of Marine Science, University of Otago, 9016 Dunedin, New Zealand

⁶Earth Sciences New Zealand, 6021 Wellington, New Zealand

⁷Department of Biology, University of Antwerp, 2610 Wilrijk, Belgium

*Corresponding author. Department of Marine Science, University of Otago, 9016 Dunedin, New Zealand. E-mail: [REDACTED]

Abstract

Anthropogenic activities that disturb the seafloor inadvertently affect the organic carbon cycle. Mobile bottom-contacting fishing (MBCF) is a widespread fishing technique that involves the dragging of fishing gear across the seafloor and disrupts seafloor sediments and alters carbon storage dynamics. However, the impact of MBCF on carbon sequestration is still not well quantified, with global estimates of MBCF-induced carbon release ranging from less than 17 Mt C yr⁻¹ to 400 Mt C yr⁻¹ with limited assessment of associated uncertainties. Addressing these knowledge gaps is essential for informing effective, evidence-based policy. Here, we force a carefully parametrized organic carbon mineralization model with empirical relationships and observational data from the Northwest European continental shelf and use a Monte-Carlo approach to assess the uncertainty associated to our estimate. We find that MBCF on the Northwest European continental shelf could reduce sedimentary carbon storage by 270 kt C yr⁻¹. However, the estimated uncertainty remains large (25%-75% percentile range = 620 kt C yr⁻¹), mainly due to uncertainties in the spatial variability of organic carbon reactivity. Our findings also show that the divergence of carbon release estimates in the literature is primarily due to differences in how organic carbon reactivity is parameterized, with higher release estimates often reflecting overestimated mineralization rates. Overall, our study demonstrates the need for targeted experimental studies to quantify how sediment disturbance influences organic carbon reactivity, to better constrain the impacts of anthropogenic activities on the marine carbon cycle and support accurate carbon accounting and informed policymaking.

Keywords: bottom trawling; mobile bottom-contact fishing; seafloor; organic carbon

Introduction

As an important organic carbon (OC) store and sink, the seafloor plays an essential role in the global carbon cycle (Berner 1982). The upper 10 cm of the global seafloor stores between 170 and 320 Gt OC, of which ~10% is located within the continental margin (Lee et al. 2019, LaRowe et al. 2020). In addition, the global seafloor removes between 130 and 350 Mt C yr⁻¹ from the fast-cycling carbon pool by burying it deep in marine sediments where it is sequestered for long timescales (Berner 1982, Hedges and Keil 1995, Keil 2017, LaRowe et al. 2020).

Anthropogenic pressure on the marine and in particular the coastal environment has been increasing in recent years (Halpern et al. 2019) and the development of reliable estimates of carbon loss has been identified as one of the 15 key issues in a horizon scanning exercise for conservation (Sutherland et al. 2024). One of the most disturbing anthropogenic pressures on continental shelves is mobile bottom-contacting fishing (MBCF), which includes activities such as bottom trawling, seining, and dredging for fish and shellfish (Halpern et al. 2008, Eigaard et al. 2017, Amoroso et al. 2018), due to both its intensity and its global occurrence (ap-

proximately 15% of the continental shelf surface is disturbed by MBCF; Amoroso et al. 2018b). MBCF physically impacts sediment dynamics in two distinct ways: (i) by resuspending (and relocating) the surface layer of the seafloor and (ii) by mixing the upper few centimetres of the seafloor (Churchill 1989, Pilskaln et al. 1998, O'Neill and Ivanovic 2016, O'Neill and Summerbell 2016, Hiddink et al. 2017, Depestele et al. 2019, Pitcher et al. 2022).

Because surface continental shelf sediments contain relatively high amounts of particulate organic carbon (POC) and contribute an estimated ~80% to the global OC burial flux (Burdige 2007, LaRowe et al. 2020), MBCF can have an important impact on POC storage and burial in the seafloor (Tiano et al. 2024a, Paradis et al. 2019, Sala et al. 2021, Epstein et al. 2022, Porz et al. 2024). Existing field data and modelling studies suggest that the resuspension and relocation of the surface sediment after a MBCF event decreases the in-situ sedimentary POC mineralization and burial through the physical removal of POC in the top layer (Tiano et al. 2019, De Borger et al. 2020). However, at the same time, the resuspended POC is likely mineralized faster in the water column, either through re-exposing this previously buried POC to

oxygen (Middelburg and Levin 2009, LaRowe and Van Cappellen 2011), and/or by removing the particles from the sediment matrix, which can potentially lead to a destabilization of organo-mineral associations, making the POC tentatively more susceptible to mineralization (Hedges and Keil 1995, Arnarson and Keil 2001). The mixing of the upper (< 10 cm) sediment layers also potentially stimulates POC mineralization (van de Velde et al. 2018) through the introduction of oxygenated water into the previously deeper, anoxic sediment layers (LaRowe and Van Cappellen 2011, Arndt et al. 2013, van de Velde et al. 2018) or priming, where the mixing of more reactive POC with less reactive POC enhances the breakdown of the latter (Zhu et al. 2024). It has thus been suggested that MBCF-induced sediment perturbations increase overall POC mineralization and carbon release while decreasing POC burial in comparison to undisturbed sediments.

There is disagreement in the literature, however, on the excess mineralization (i.e. additional carbon release caused by MBCF in comparison to carbon release from undisturbed sediments) of this anthropogenic perturbation (Sala et al. 2021, Epstein et al. 2022, Hiddink et al. 2023, Atwood et al. 2024). Recent estimates proposed that global MBCF is responsible for the additional mineralisation of $200\text{--}400\text{ Mt C yr}^{-1}$ globally (Sala et al. 2021, Atwood et al. 2024), but this estimate has been debated and it has been suggested it overestimates the excess mineralization by 1–2 orders of magnitude (Hiddink et al. 2023). A more recent coupled hydrodynamic-biogeochemical modelling study of the North Sea estimates that MBCF reduces POC burial in the sediment by $\sim 1.0\text{ t C km}^{-2}\text{ yr}^{-1}$, which upscales to a mere $\sim 10\text{ Mt C yr}^{-1}$ reduction in global POC burial (Porz et al. 2024, Zhang et al. 2024). The stark discrepancy between these mineralization estimates likely stems from a series of oversimplifying assumptions underlying the Sala et al. (2021) and Atwood et al. (2024) estimates, in combination with the lack of consideration for sources of uncertainty in the different model estimates (Hiddink et al. 2023). The current disagreement around the impact of MBCF on coastal POC is critical given the prominent discussion of the impact of MBCF on carbon release and its role in national carbon accounting. Evidence-based policy making, as well as coastal management requires a robust assessment of the impact on carbon stocks and burial (Vanderklift et al. 2022).

The aim of this paper is twofold. Firstly, we want to show that a parametrization of the “1G” OC mineralization model approach used by Sala et al. (2021) and Atwood et al. (2024) based on an ensemble of published, empirically-derived model parameters leads to mineralization estimates that fall close to the 3D model estimates of Zhang et al. (2024) and Porz et al. (2024). Secondly, we apply a Monte Carlo approach to estimate the uncertainty associated with these estimates. We identify the main sources of this uncertainty and thus provide a guide for future research and experimental efforts required to reduce these uncertainties. Here, we focus on the north-west (NW) European continental shelf, which is one of the most extensively studied coastal regions. The available comprehensive and interdisciplinary observational dataset that is available for this region enables us to better constrain model parameters and forcings, thus allowing for a robust quantification of the impact and associated uncertainty of MBCF on sediment relocation and mixing and ultimately additional carbon release.

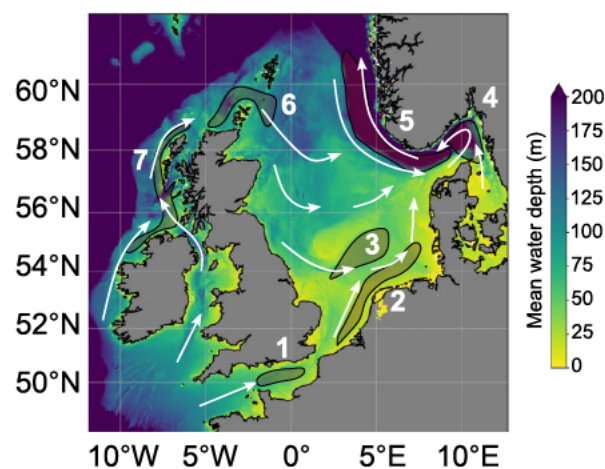


Figure 1. Northwest European shelf bathymetry with an indication of the general current patterns (white arrows) and 7 accumulation areas for particles released at the sea surface [based on (Turrell 1992, Ricker and Stanev 2020)]. 1 = English Channel, 2 = Southern and German Bight, 3 = south of Dogger Bank, 4 = Skagerrak, 5 = Norwegian trench, 6 = Fair Isle Current, 7 = northern coast of Ireland and Great Britain.

Materials and methods

Study area

The NW European continental shelf covers a surface area of 1.1 million km^2 (Wilson et al. 2018, Legge et al. 2020) and borders several European countries: Norway, Sweden, Denmark, Germany, the Netherlands, Belgium, France, Ireland, and the United Kingdom. NW European shelf waters are characterized by a shallow, well-mixed water column in the east and south and deep seasonal stratification in the north. The NW European shelf is connected to the open ocean in the North and West. Natural resuspension and currents transport particles mainly via three distinct pathways (Fig. 1; Turrell 1992, Emeis et al. 2015). Particles enter the area via the English Channel and are transported along the Southern and German bights up to the Skagerrak (Fig. 1). Alternatively, currents flowing from the east and west of Ireland, converge on the west side of the Outer Hebrides and enter with the Fair Isle current into the North Sea. Water inside the NW European shelf moves to the east, either via the south of the Dogger Bank, through the middle of the North Sea, or across the Fladen Ground. On the east side, a cyclonic current moves material to the Skagerrak and eventually into the Norwegian trench (Fig. 1). Along the NW European shelf's main flow pathways, 7 major depositional areas can be delineated (note that these areas have been identified based on particles released at the surface; Ricker and Stanev 2020): the English channel, the Southern and German Bight, south of Dogger bank, Skagerrak, the Norwegian trench, Fair isle current and Fladen grounds, and the Outer Hebrides (Fig. 1). However, except for the Norwegian trench, all of these depositional areas can be considered transient depositional zones (de Haas et al. 1997, Diesing et al. 2021), which results in rather low accumulation rates of material across the whole NW European shelf, compared to the high accumulation rates in the Norwegian trench (Diesing et al. 2021).

The NW European continental shelf seafloor is dominated by sandy sediments and the distribution of sediment types is largely determined by hydrodynamics and bathymetry

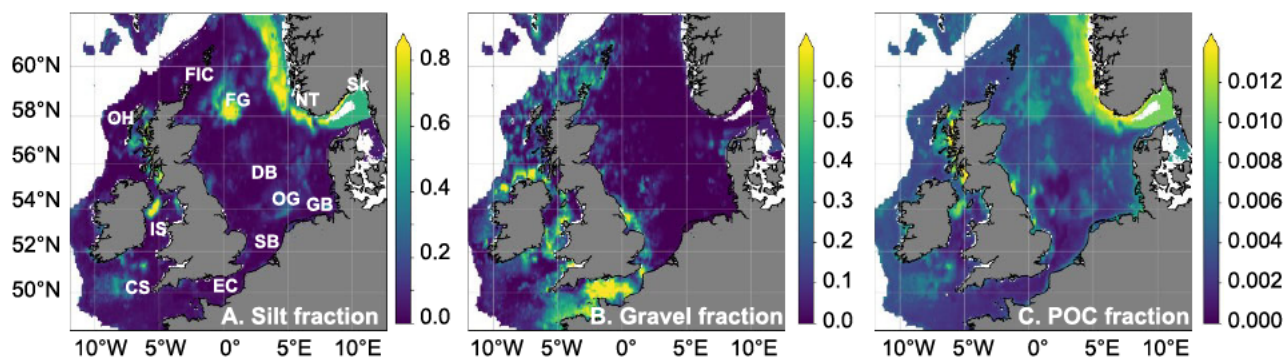


Figure 2. A Fraction of silt (grain diameter < 0.06 mm) in the top ~10 cm of the seafloor, with an indication of the main areas discussed in the text (starting from the bottom left, going anti-clockwise); CS = Celtic Sea, EC = English Channel, SB = Southern Bight, OG = Oyster Grounds, GB = German Bight, DB = Dogger Bank, Sk = Skagerrak, NT = Norwegian Trench, FG = Fladen Ground, FIC = Fair Isle Current, OH = Outer Hebrides, IS = Irish Sea. B Fraction of gravel (grain diameter > 2 mm) in the top ~10 cm of the seafloor. C Fraction of particulate organic carbon (POC) in the top ~10 cm of the seafloor (data from (Wilson et al. 2018)).

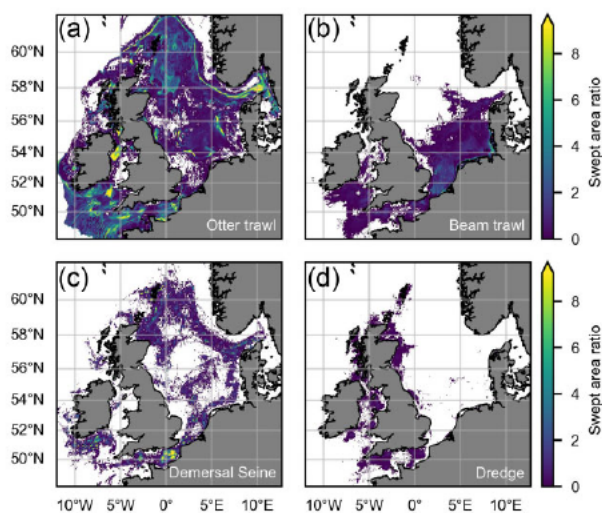


Figure 3. Map of the NW European continental shelf with an indication of the mean annual total MCBF intensity ("swept area ratio," i.e. the number of times the surface of a given pixel is completely disturbed by MCBF gear per year) for (a) Otter trawl, (b) Beam trawl, (c) Demersal seine, and (d) Dredge over the period 2009–2017. MCBF data was retrieved from ICES (ICES 2021).

(Bockelmann et al. 2018, Wilson et al. 2018). In the shallow waters (~20 m) of the Strait of Dover and the English Channel, intense shear stress leaves coarse sands behind and suspends finer materials that are transferred along the eastern border through the East Anglian turbidity plume and are deposited in the Skagerrak (Fig. 2A, B). Deposition of finer sediments also occurs in regions of low current speeds, such as Fladen Ground, the Oyster Grounds, and the Norwegian Trench (Eisma and Kalf 1987, Diesing et al. 2021) (Figure 2A). Because OC adsorbs on silt particles, the POC distribution in the NW European shelf generally follows these main patterns of silt distribution (Diesing et al. 2021) (Figure 2A, C).

As one of the most productive shelf seas (Steinacher et al. 2010), the NW European continental shelf is intensively fished with local MCBF frequencies exceeding 10 passes over a given area of seabed, on average, per year (Fig. 3; Eigaard et al. 2017, Amoroso et al. 2018b; ICES 2024). Nearly 6600 fishing vessels trawl and dredge in the NW European continental shelf,

with total landings in 2010–2012 of around 922 000 metric tons (Amoroso et al. 2018). Vessels that are active in European waters use four main demersal mobile gear types: otter trawls, beam trawls, seines, and dredges (Eigaard et al. 2017). Beam trawling activity is typically higher in the southern North Sea, while otter trawling activity is more active in the northern North Sea, the Skagerrak, and the Celtic Seas. Bottom seine fishing is practiced more often in the English Channel and to a lesser extent in the North Sea (Fig. 3; ICES 2022). Dredge fisheries are used for scallops, mainly in the English Channel and UK territorial waters. Dredges and flatfish-targeting beam trawls have a smaller swept area by hour fishing than otter trawls, demersal seines, and shrimp-targeting beam trawls (Eigaard et al. 2016), but penetrate the sediment deeper (Hidink et al. 2017, Pitcher et al. 2022). These MCBF gears contact the seabed surface at least once per year in 18% of the surface area of the Norwegian trench and in > 65% of the surface areas of the Channel, the Southern and Central North Sea (Matear et al. 2023).

Spatial distribution of organic carbon and mobile bottom-contact fishing activity in the NW European Shelf

Our analysis is based on the MCBF data for the years 2009–2017 provided by the International Council for the Exploration of the Sea (ICES 2021). This dataset provides the swept area (SA, the area of a grid cell that is fished every year) as well as the swept-area ratio (SAR, the number of times the surface of the whole grid cell is fished per year) at a resolution of $0.05^\circ \times 0.05^\circ$ (Fig. 3). Both SA and SAR are calculated from gear characteristics and the vessel monitoring system (VMS) data using the methodology of Eigaard et al. (2017), while gear penetration depths were derived from the MCBF type and sediment type following Pitcher et al. (2022) (see below for details). Note that this dataset does not contain vessels smaller than 12 meters in length, since they are not required to use VMS.

Silt content (% dry weight), gravel content (% dry weight), and POC content (% dry weight) for the NW European continental shelf sediment were inferred from the synthetic maps presented in (Wilson et al. 2018) (Figure 2). These maps are based on existing survey data and statistical models of bed shear stress and bathymetric properties. Because the

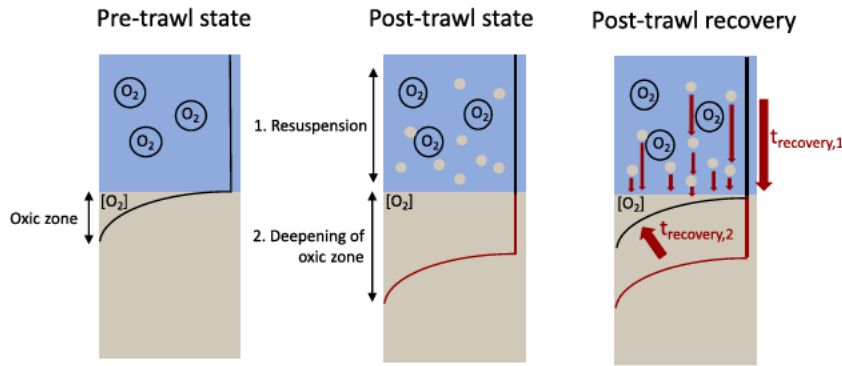


Figure 4. Conceptual image of MBCF on the seafloor. In its undisturbed state, oxygen only penetrates a few centimetres into the sediment. When a MBCF gear passes by; (1) part of the sediments gets resuspended into the oxygenated overlying water and (2) oxygen gets introduced into the previously anoxic part of the sediment. We consider two timescales of recovery, the time it takes for the resuspended particles to settle out of the water column ($t_{\text{recovery},1}$) and the time it takes for oxygen penetration to recover to its initial level ($t_{\text{recovery},2}$).

resolution of these maps was coarser than the resolution of the MBCF data ($0.125^\circ \times 0.125^\circ$), the sediment property data was linearly interpolated to the same resolution as the MBCF dataset. The total grid surface area of the map was 1 107 159 km², which is the surface area we use in further calculations.

Quantifying mobile bottom-contact fishing induced POC mineralization and carbon release

Organic carbon mineralization model

To estimate the amount of OC that is additionally mineralized because of a MBCF-induced disturbance, we applied a 1 G organic carbon mineralization model (Berner 1980, Arndt et al. 2013) that is identical to the one used in previous studies (Sala et al. 2021). However, we here used a different model parameterization. The 1 G model assumes that OC is mineralized according to a first-order rate law. The total amount of POC mineralized at a given location over time t (R_{min} , in kg) is given by (Berner 1980)

$$R_{\text{min}} = - \int_{t=0}^t C_0 e^{-kt} dt = C_0 (1 - e^{-kt}) \quad (1)$$

Where C_0 is the amount of POC at time zero (in kg), k is the first-order rate constant (in yr⁻¹) and t is the time (in yr). The first-order rate constant, k is a measure of the apparent OC reactivity. It is influenced by different factors, such as the type or origin of the organic carbon, its mineralization and transport history, the availability of terminal electron acceptors, organo-mineral interactions, and microbial community structure. A large body of empirical data shows that k typically decreases with mineralization time (Middelburg et al. 1997). However, the use of this simple single-component one-pool OC mineralization model with a constant mineralization constant is justified here because the duration of the MBCF-disturbance spans hours to days (as explained below), allowing us to treat reactivity as constant over this short timespan (Arndt et al. 2013).

To estimate the amount of additional POC mineralization that occurs because of MBCF (i.e. exceeding the mineralization of POC in an undisturbed sediment), we need to estimate by how much MBCF disturbance increases R_{min} . This increase can be calculated by the difference between the total R_{min} under disturbed conditions and R_{min} that would occur without

disturbance, i.e.

$$\begin{aligned} R_{\text{min},\text{trawling}} &= R_{\text{min},\text{disturbed}} - R_{\text{min},\text{undisturbed}} \\ &= C_{\text{dist}} \left(1 - e^{-k_{\text{disturbed}} t_{\text{recovery}}} \right) \\ &\quad - C_{\text{dist}} \left(1 - e^{-k_{\text{undisturbed}} t_{\text{recovery}}} \right) \\ &= C_{\text{dist}} \left(e^{-k_{\text{undisturbed}} t_{\text{recovery}}} - e^{-k_{\text{disturbed}} t_{\text{recovery}}} \right) \end{aligned} \quad (2)$$

Where $k_{\text{undisturbed}}$ is the first-order decay constant under undisturbed conditions, $k_{\text{disturbed}}$ the first-order decay constant under disturbed conditions, C_{dist} the amount of POC disturbed, and t_{recovery} the time it takes for the local sediment conditions to recover from the disturbance event (Fig. 4).

Furthermore, the disturbing effect of MBCF can be divided into its two distinct physical impacts: resuspension of an affected sediment layer and mixing of an affected sediment layer (Fig. 4):

$$\begin{aligned} R_{\text{min},\text{resuspension}} &= C_{\text{dist},\text{resuspension}} \left(e^{-k_{\text{undisturbed}} t_{\text{recovery},1}} - e^{-k_{\text{disturbed}} t_{\text{recovery},1}} \right) \end{aligned} \quad (3)$$

$$R_{\text{min},\text{mixing}} = C_{\text{dist},\text{mixing}} \left(e^{-k_{\text{undisturbed}} t_{\text{recovery},2}} - e^{-k_{\text{disturbed}} t_{\text{recovery},2}} \right) \quad (4)$$

Below, we discuss how to constrain (i) the first-order decay constant under undisturbed and disturbed conditions ($k_{\text{undisturbed}}$ and $k_{\text{disturbed}}$), (ii) the amounts of POC affected by resuspension and mixing ($C_{\text{dist},\text{resuspension}}$ and $C_{\text{dist},\text{mixing}}$), and (iii) the timescale of recovery from resuspension and mixing ($t_{\text{recovery},1}$ and $t_{\text{recovery},2}$).

Apparent POC reactivity for undisturbed and disturbed conditions

Apparent OC reactivity is a critical but difficult-to-constrain model parameter, as it implicitly accounts for all the factors that control POC reactivity (Arndt et al. 2013). Typical first-order mineralization rate constants for OC reaching the surface of coastal sediments range from 10^{-3} to 10^2 yr⁻¹ (Arndt et al. 2013). However, the POC reactivity generally decreases

with mineralization time and burial depth. This widely observed decline in reactivity is often particularly pronounced in shallow shelf sediments, where the deposited bulk OC mix still includes highly reactive compounds that are rapidly consumed in the upper mixed layer. Average first-order mineralization rate constants representative of POC within the upper diagenetic sedimentary layers will thus be 1–2 orders of magnitude lower, and typically range from 10^{-4} to 10^1 yr^{-1} with a peak around 10^{-2} yr^{-1} (Arndt et al. 2013, Freitas et al. 2021). These rate constants represent the apparent reactivity of the bulk POC within the mixed layer of the sediment (i.e. shallower than 10 cm). Here, we assume that, if not disturbed, organic matter within the upper layers of NW European shelf sediments degrades with first-order rate constants $k_{\text{undisturbed}} = 10^{-4} - 10^1 \text{ yr}^{-1}$. This range spans the entire range of first-order rate constants reported for global continental shelf sediments (Arndt et al. 2013, Freitas et al. 2021). This is a robust assumption, but nevertheless highlights the large uncertainty associated with the heterogeneity of shelf environments that translates into apparent rate constants that differ over several orders of magnitude.

MBCF can affect apparent organic carbon (and thus k) reactivity through enhanced oxygen exposure either by (i) resuspension of sediment into the oxygenated water column and (ii) the injection of oxygen into previously anoxic parts of the sediment via the mixing of sediment (Fig. 4). In both cases, the net effect of this disturbance is that the exposure of sedimentary organic matter to oxygen is prolonged compared to the undisturbed scenario. Observational data suggest that such a prolonged oxygen exposure time will have an important impact on organic matter reactivity and thus mineralization. Many empirical studies have shown that the total amount of organic carbon mineralized in the upper sediments strongly and positively correlates with the length of time organic matter is exposed to oxygen in sediment pore waters (Hartnett et al. 1998, Middelburg and Levin 2009). Different mechanisms may explain this link. First, prolonged exposure to oxygen can directly stimulate the mineralization of the structurally more complex and thus less reactive POC compounds as shown by several field and theoretical studies (Middelburg and Levin 2009, LaRowe and Van Cappellen 2011). Additionally, apparent POC reactivity is controlled by the dynamic interplay of different environmental factors, such as the presence of reactive clay surfaces, iron oxides, bioturbation, or feeding by benthic fauna that are all influenced by oxygen availability (Canfield 1994, Mayer 1994, Burdige 2007, Arndt et al. 2013). Oxygen exposure time thus seems to be an effective measure that encapsulates this complex interplay of environmental controls on POC reactivity and thus mineralization rates (Hartnett et al. 1998, Middelburg and Levin 2009). In line with this large body of empirical and theoretical evidence, we assume that the prolonged oxygen exposure times following a MBCF-induced physical sediment disturbance will enhance organic matter mineralization through increasing organic matter mineralization rate constants. A first estimate of such an increase can be derived by comparing first-order reactivity constants for POC mineralization under oxic and anoxic conditions. Based on the global compilation by Katsev and Crowe (2015), we assume that a re-exposure of organic matter to oxic conditions could increase the NW European shelf sediment constants by a factor of 1–5, which aligns with experiments done in the Kiel Bight (Kalapurakkal et al. 2025a). Note that most of the oxic mineralization constants

of Katsev and Crowe (2015) were derived from POC mineralization in the water column, while the anoxic mineralization constants were derived in the sediment. This assumed increase in first-order mineralization rate constants upon disturbance integrates, besides the increased availability of the thermodynamically more favourable electron acceptor oxygen, multiple environmental factors such as priming via the injection of more reactive compounds in the deeper sedimentary layers, potential desorption of POC from the mineral matrix, and/or microbial and microbenthic community changes, and associated changes in metabolic capabilities (Hedges and Keil 1995, Burdige 2007, Kaiser and Hiddink 2007, van Nugteren et al. 2009, van de Velde et al. 2018, Zhu et al. 2024).

Quantification of the amount of sediment and particulate OC impacted by mobile bottom-contact fishing

Resuspension

For each grid cell, we quantified the amount of sediment resuspended per square metre of seabed swept by a passing MBCF gear (S_R , in kg m^{-2}) using the empirical relation between mass resuspended, the hydrodynamic drag created by the gear components (D_c , in N m^{-1}) and the silt fraction of the sediment (s_f , unitless) (O'Neill and Summerbell 2011, Rijnsdorp et al. 2021, Breimann et al. 2022),

$$S_R = 2.602s_f + 1.206 * 10^{-3}D_c + 1.321 * 10^{-2} s_f D_c \quad (5)$$

The dataset of Wilson et al. (2018) was used to determine s_f (Fig. 2A). The hydrodynamic drag D_c of the gear components of the beam trawl was taken from Rijnsdorp et al. (2021) and was divided into small ($\leq 221 \text{ kW}$) and large ($> 221 \text{ kW}$) vessels. The hydrodynamic drag for the gear components of the otter trawl was taken from O'Neill and Summerbell (2011) and is representative of gear towed by a 1000–1400 horsepower vessel in the Scottish demersal whitefish fleet. Hydrodynamic drag of wire sweeps for otter trawl was approximated by the drag created by seine ropes of 26 mm diameter (O'Neill and Noack 2021). The trawl net for otter trawl was estimated from the empirical relationship between the twine surface area A of the bottom net panels (Polet and Fonteyne 1995, Palder et al. 2023) and fishing speed U of 2.9 knots (Eigaard et al. 2016) as reported in (Reid 1977) :

$$D_c = \frac{0.5\rho * U^2 * A * 0.643}{1 + 0.923U} \quad (6)$$

Twine surface area is estimated from the number of meshes at the top of the panel (N_t), at the bottom of the panel (n_b), the number of meshes in the height of the panel (H), the mesh size (a) and the twine diameter (d_t) using (Prado 1990):

$$A = \frac{\frac{(N_t + n_b)}{2} * H * 2(a * d_t)}{1e6} \quad (7)$$

For seines, we assumed that netting material and cod-end constructions were similar as for beam trawls (Noack et al. 2017), though with operation at speeds of ~ 1 knot (Eigaard et al. 2016, O'Neill and Noack 2021). The drag created by the seine rope was taken from (O'Neill and Noack 2021). Hydrodynamic drag of dredges was estimated using Eq. (5) and empirical resuspension estimates of 0.85 kg m^{-2} in a habitat with 4.1% silt content (O'Neill et al. 2013) (Table 1), which is three to five times less than resuspension in a beam trawl experiment (Depestele et al. 2016). A single dredge is $\sim 80 \text{ cm}$ in width, and a typical scallop dredge operates with 8 dredges on each side (O'Neill et al. 2013), which leads to a total gear

Table 1. Parameters used in eq. (5) and (8). Drag (D_c) and footprint of the individual gear components are reported with 1 s.d. (where available). We assumed all beam trawls had tickler chains. Footprint is reported as mean \pm 1 standard deviation, with the range of the available data given in square brackets. For the seine footprint, there was only an estimated value available, so we assumed a possible range of \pm 5%. Gear penetration depth is reported with the 1 standard deviation (where available). Where no standard deviation was reported, we assumed a normal distribution with a standard deviation of 50% of the mean value, except for the penetration depth of the seine, where we assumed a uniform distribution due to limited data availability. Distributions are shown in Fig. S1-S5

Otter trawl	Hydrodynamic drag D_c ($N\ m^{-1}$)			
	Trawl door	Sweeps	Ground gear	Bottom net panels
Footprint (%)	4020 ^a 1.9 \pm 1.8 ^c [0.8, 3.7]	0.675 ^b 73 \pm 47 ^c [29.2, 100]	1165.6 ^a 25 \pm 32 ^c [5.0, 55.5]	381 ^b 25 \pm 32 ^c [5.0, 55.5]
Beam trawl	Shoes	Ticklers	Ground gear	Bottom net panels
Small vessels	19 ^d	699 \pm 194 ^d	135 \pm 115 ^d	1595 \pm 805 ^d
Large vessels	13 \pm 2 ^d	2118 \pm 352 ^d	572 \pm 140 ^d	1967 \pm 333 ^d
Footprint (%)	6.3 \pm 4.0 ^c [2.2, 11.7]	93.7 \pm 4.0 ^c [88.3, 97.7]	93.7 \pm 4.0 ^c [88.3, 97.7]	93.7 \pm 4.0 ^c [88.3, 97.7]
Demersal seine		Seine rope	Ground gear	Bottom net panels
Footprint (%)		0.675 ^e 90 ^c [85, 95]	1165.6 ^a 10 ^c [5, 15]	70 ^b 10 ^c [5, 15]
Dredge	Dredge	Nr of dredges	Total drag	
Footprint (%)	42.5 ^b	6–30 ^b	255–1275 ^b 100 ^c	
Gear penetration depth PD (cm)				
	Mud	Sand		
Otter trawl	2.0 \pm 6.6 ^f	1.1 \pm 5.0 ^f		
Beam trawl	3.2 \pm 1.7 ^f	1.9 \pm 1.9 ^f		
Demersal seine	0.0–2.0 ^g	0.0–1.1 ^g		
Dredge	5.4 \pm 9.0 ^f	3.5 \pm 6.1 ^f		

^a(O'Neill and Summerbell 2011), no standard deviation was reported.

^bEstimated (see main text).

^c(Eigaard et al. 2016), no standard deviation was reported for the footprint of individual gear components of a seine.

^d(Rijnsdorp et al. 2021).

^e(O'Neill and Noack 2021).

^f(Hiddink et al. 2017, Pitcher et al. 2022).

^gTable 3 in (Szostek et al. 2022) for otter trawl without doors, which we assumed is comparable to seine rope. We assumed a uniform distribution between observed minimum and maximum in muddy or sandy sediments.

width of \sim 13 m. The range of dredge gear widths for different vessels is 5 m–25 m (Eigaard et al. 2016), which suggests that the number of dredges per vessel ranges between 6 and 30, which is the uncertainty range we use (Table 1). The results from individual gears are upscaled from empirical experiments, and our results are therefore less suitable for comparing individual gear impacts. Another simplifying assumption we make is that all beam trawls have tickler chains, which would lead to an overestimation of the total beam trawl impact. The sediment resuspended was first calculated for each gear component, and a weighted sum was calculated per grid cell using the typical fraction the gear represents in the total footprint of the gear (Eigaard et al. 2016). Differences in penetration depth were not accounted for, following the methodology in Rijnsdorp et al. (2021).

To obtain the total amount of sediment resuspended annually per grid cell (TS_R), we multiplied the annual swept area of each gear with its respective amount of sediment resuspended per swept area,

$$TS_R = S_R * SA \quad (8)$$

To estimate the amount of POC resuspended ($C_{dist, resuspension}$ in Eq. (3)), TS_R was multiplied with the predicted surface (<10 cm) POC concentration (in $g\ POC\ g^{-1}$ sediment) of the grid cell (Fig. 2C). We thus implicitly assumed that the POC

content of resuspended material is equal to the average POC content in the upper 10 cm.

The timescale of the impact of resuspension ($t_{recovery,1}$ in Fig. 4 and Eq. (3)) can be estimated from the resuspension height of a sediment particle (h_{plume} , in m) (i.e. the height of the plume after a MBCF gear passed) and the settling velocity of this particle ($u_{settling}$, in $m\ yr^{-1}$)

$$t_{recovery,1} = \frac{h_{plume}}{u_{settling}} \quad (9)$$

Mixing

In addition to eroding surface sediments, a passing MBCF gear also mixes the top layers of the sediment down to a certain depth. The amount of sediment that is mixed per square metre of seabed swept by a passing MBCF gear (S_m , in $kg\ m^{-2}$) can be estimated as,

$$S_m = \rho_{sed} (1 - \varphi) (PD * 10^{-2}) \quad (10)$$

where ρ_{sed} is the sediment density ($2600\ kg\ m^{-3}$), φ is the porosity of the sediment (0.8 for mud, and 0.4 for sand), and PD is the penetration depth of the gear (cm). Penetration depths for all types of gears were determined as a function of gear and the sediment type (Table 1; Pitcher et al. 2022). We specified the spatial distribution of gear penetration depths

Table 2. Parameter ranges and their assumed distribution for the organic carbon mineralization model. Details are given in the text and distribution plots are shown in Fig. S6

	range	Unit	distribution	reference
$k_{undisturbed}$	10^{-4} – 10^{-1}	yr^{-1}	logarithmic	(Arndt et al. 2013, De Borger et al. 2021, Freitas et al. 2021)
$k_{disturbed}$	$1k_{natural} - 5k_{natural}$	yr^{-1}	uniform	(Katsev and Crowe 2015)
h_{plume}	0–6	M	logarithmic	(Durrieu de Madron et al. 2005)
$u_{settling}$	10^{-4} – 10^{-4}	m d^{-1}	logarithmic	(McCandliss et al. 2002)
$[\text{O}_2]_{homog}$	0.3	$\mu\text{mol cm}^{-3}$	-	
R_{vol}	2–200	$\mu\text{mol cm}^{-3} \text{yr}^{-1}$	logarithmic	(Soetaert et al. 1996, Burdige 2007)

following Pitcher et al. (2022) and using the data in Fig. 2A, B. Specifically, if the cell contained more than 50% of gravel, we assumed that $PD = 0$, if the cell contained more than 50% silt, the penetration depth in muddy sediment was chosen, in all other cases we chose the penetration depth in sandy sediment. To obtain the total amount of sediment mixed annually per grid cell (TS_M), we multiplied the annual swept area of each gear with its respective amount of sediment mixed per swept area,

$$TS_M = S_M * SA \quad (11)$$

The amount of POC mixed ($C_{dist,mixing}$ in Eq. (4)), was then derived by multiplying TS_M with the POC content (Fig. 2C). Not all the gear will penetrate the seafloor, which means our mixed sediment estimate is an overestimation.

We estimate the recovery timescale of the sediment mixing impact ($t_{recovery,2}$ in Fig. 4 and Eq. (4)), by first calculating the amount of oxygen that is injected into the sediment ($O_{2,inj}$) in the sediment as:

$$O_{2,inj} = \varphi * [\text{O}_2]_{homog} * PD \quad (12)$$

Where $[\text{O}_2]_{homog}$ is the oxygen concentration (in $\mu\text{mol cm}^{-3}$) after a MBCF gear passed. We hereby assume that the oxygen penetration depth (OPD) in an undisturbed shelf sediment is negligible compared to the penetration depth of the MBCF gear. This assumption is a good approximation in coastal sediments where OPDs are generally on the order of millimetres (Glud 2008), but we will overestimate $O_{2,inj}$ for sediments further offshore or sandy sediments that are generally characterized by OPDs of around a couple of centimetres. Additionally, waves and current transport create advective flow in sandy sediments, which can further increase oxygen penetration (Precht et al. 2004). Hence our estimated $t_{recovery,2}$ (eq. 11) should be considered a higher-end estimate. Next, we need to calculate the time it takes to consume all the newly injected oxygen, which will depend on the oxygen consumption rate of the sedimentary layer that is mixed. The oxygen consumption rate can be estimated by the volumetric mineralization rate (R_{vol} , in $\mu\text{mol cm}^{-3} \text{yr}^{-1}$) and the penetration depth PD ,

$$t_{recovery,2} = \frac{O_{2,inj}}{R_{vol} * PD} \quad (13)$$

Estimated depth-integrated POC mineralization rates (R_{int}) in shelf sediments fall into the range between 1 and 100 $\text{mmol m}^{-2} \text{d}^{-1}$, with an average of $\sim 10 \text{ mmol m}^{-2} \text{d}^{-1}$ (Middelburg et al. 1997, Burdige 2007). Because both POC content and reactivity rapidly decrease in the upper sediment, most of the POC mineralization takes place in the upper 15 cm (Soetaert et al. 1996, Freitas et al. 2021). Together, this yields

a $R_{vol}(= R_{int}/15\text{cm})$ between 2 and 200 $\mu\text{mol cm}^{-3} \text{yr}^{-1}$. Because the $t_{recovery,2}$ estimate only considers the time required to consume all newly introduced O_2 , it implicitly assumes that MBCF-induced mixing only stimulates mineralization by introducing additional oxygen into the sediment. In reality, additional factors, such as the mixing of more reactive fractions of surface POC with less reactive fractions found at depth (“priming”) or changes in the physical protection of POC could also influence POC mineralization (van Nugteren et al. 2009, Bianchi 2011, Aller and Cochran 2019, Zhu et al. 2024). However, even under undisturbed conditions, coastal and shelf sediments are generally subject to natural, continuous forms of sediment mixing (e.g. bioturbation by benthic fauna, natural resuspension events due to storms) (Aller and Cochran 2019, van de Velde et al. 2020, Tiano et al. 2024b), and MBCF-induced mixing, given this natural mixing, will likely have little long-term impact (Rooze et al. 2024).

Uncertainty estimation

To provide a robust assessment of the influence of the parameter uncertainties on our model estimates, we run a large model ensemble of 10 000 runs (the median solution was found to converge after this number of iterations; Fig. S7) over the entire plausible model parameter space (Table 1 and Table 2) sampled with a Monte Carlo method. The sampled distribution of each model parameter is shown in Fig. S1–S6. To exclude outliers caused by extreme parameter choices, we removed any results that fall outside of 3 standard deviations for the Gaussian (normal) distributions, were below 0, or fell outside the parameter ranges given in Table 2 for uniform and logarithmic distributions.

The result distribution of all ensemble runs was checked for normality. All data that were not normally distributed were found to be log-normal distributed. We report the median, 25% percentile, and 75% percentile for all model estimates.

Results

Mobile bottom-contact fishing induced sediment and particulate organic carbon resuspension

The estimated median annual amount of sediment resuspended by MBCF in the NW European shelf can reach more than 10 $\text{kg m}^{-2} \text{yr}^{-1}$, but is generally in the range of 0.1–10 $\text{kg m}^{-2} \text{yr}^{-1}$ (Fig. 5A). Model results indicate that MBCF-induced sediment resuspension is highest in areas with high silt content, such as the Norwegian trench, the Irish Sea, or Fladen Ground (Fig. 2A, Figure 5A), as well as in intensively

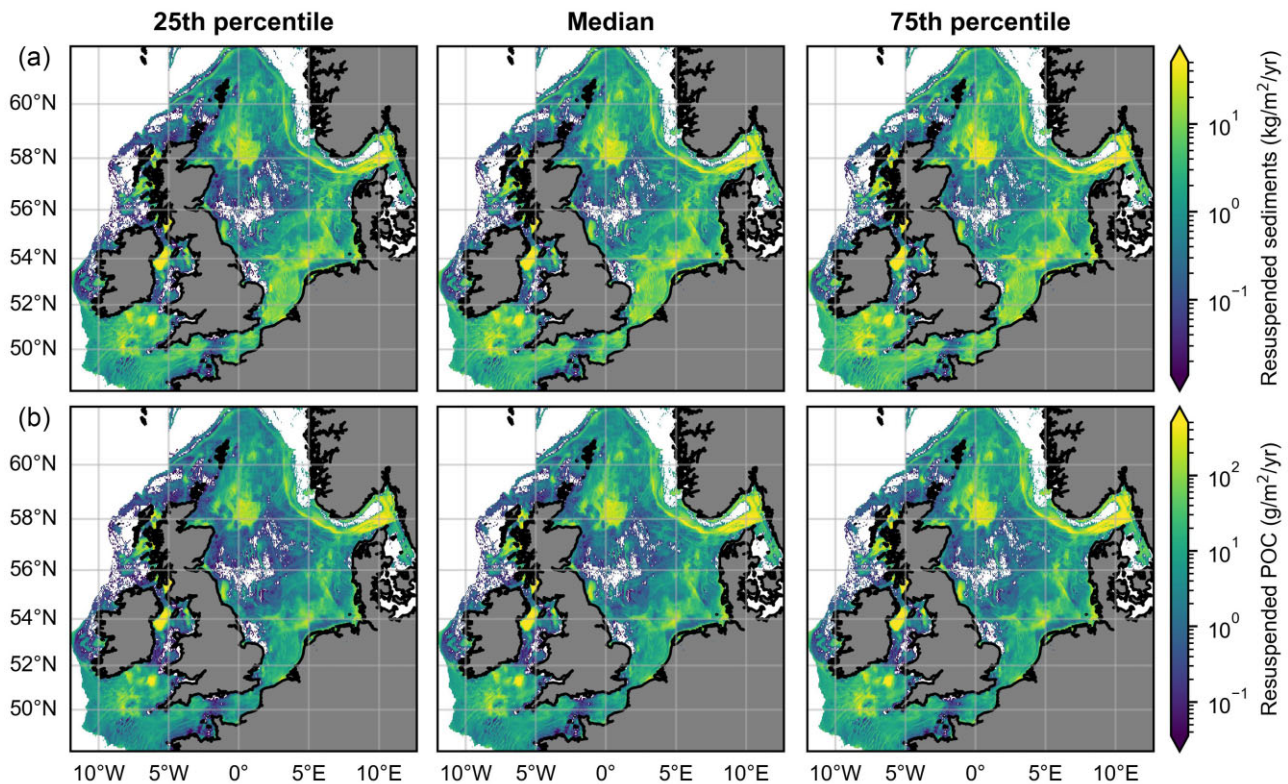


Figure 5. A Sediment resuspension and B particulate organic carbon (POC) resuspension induced by MBCF fisheries (otter, seine, beam, and dredge) in the NW European shelf for the period 2009–2017, calculated using eqs. (5) and (8) and the POC fraction shown in Fig. 2C. We show the median (left column), 25% percentile (middle column), and 75% percentile (right column) of the Monte Carlo estimate. Spatial maps of individual MBCF gears are shown in Figs. S8–S9.

fished areas, such as the Celtic Sea or the English Channel (Fig. 3, Figure 5A).

Otter trawling is by far the most widely applied MBCF technique in the NW European shelf and is responsible for more than 60% of all the sediment resuspended annually (Table 3). In contrast, dredging and demersal seine play a minor role in sediment resuspension in the NW European shelf (Table 3).

Model results highlight that the estimated amount of resuspended POC through MBCF is mainly determined by the POC concentration, and to a lesser degree by fishing intensity (Fig. 5B). The estimated amount of resuspended POC is highest (POC resuspension rates of $>100 \text{ g C m}^{-2} \text{ yr}^{-1}$) in areas with the highest surface POC content (POC $>1 \text{ wt } \%$), such as the Norwegian trench, Fladen ground, Irish Sea, and Outer Hebrides (Fig. 6B). In these muddier and, thus, POC-rich areas, otter trawling is the dominant MBCF technique and accounts for $>80\%$ of total annual POC resuspension in the NW European shelf (Table 3). In contrast, dredge fisheries are limited in scope and target areas of coarser grain sizes with lower POC content and are consequently responsible for less than 0.4% of the estimated annual POC resuspension in the NW European shelf (Table 3). Demersal seining resuspends ~ 5 times less POC than beam trawling, while its swept area is ~ 2 times larger, mainly because the seine gear creates less drag (Table 1). In the context of these comparisons, it is important to highlight again that these estimates of MBCF-induced sediment and POC resuspension are based on upscaling from a limited set of empirical studies. Future studies are required to further refine these estimates to overcome the high uncertainty of POC resuspension caused by MBCF.

Mobile bottom-contact fishing induced sediment and particulate organic carbon mixing

The spatial distribution of MBCF-induced sediment mixing does not correlate as strongly with the areas of high silt content as the MBCF-induced sediment resuspension (Fig. 6A). Results indicate that otter trawling is responsible for the largest sediment volume mixed (75 Gt yr^{-1} ; Table 3). Beam trawling is responsible for an estimated 6.6 Gt yr^{-1} , which is double the estimated mixed volume for seines (3.0 Gt yr^{-1}), due to the deeper penetration depth of the beam trawl (Table 1) and the application of seine in more sandy areas (Fig. 2 and Figure 3). Dredges only mix 1.3 Gt yr^{-1} of NW European shelf sediment, mainly due to their limited application on the NW European shelf (Fig. 3C).

Like the amount of resuspended POC, the amount of POC mixed by MBCF fishing strongly depends on the POC content. The spatial distribution of the mixed POC amount thus reflects areas of high silt (and POC) content (Fig. 6B). Model results suggest that MBCF annually mixes an estimated total median amount of 360 Mt C yr^{-1} of POC in the NW European shelf. Otter (320 Mt C yr^{-1}) and beam (20 Mt C yr^{-1}) trawling are responsible for $>90\%$ of the total annual POC mixing (Table 3).

Enhanced mineralization due to mobile bottom-contact fishing induced sediment disturbances

Model results reveal that MBCF-induced sediment mixing stimulates POC mineralization more than sediment

Table 3. Average swept area over the period 2009–2017, total annual sediment resuspension and mixing, particulate organic carbon (POC) resuspension and POC mixing in the seabed, and estimated enhanced POC mineralization for resuspension and mixing per gear type. Results are reported for 10 000 iterations. The median and percentiles of the total are calculated from the distribution that was generated after summing up the individual iterations, which explains why the sum of median values of the individual techniques does not always equal the median of the reported total. Results are reported as median [25% percentile, 75% percentile]

Gear type	Swept area ($10^3 \text{ km}^2 \text{ yr}^{-1}$)	Resuspension			Mixing		
		Total annual sediment mass (Gt yr^{-1})	Total annual POC mass (Mt C yr^{-1})	Enhanced POC mineralization (kt C yr^{-1})	Total annual sediment mass (Gt yr^{-1})	Total annual POC mass (Mt C yr^{-1})	Enhanced POC mineralization (kt C yr^{-1})
Otter	1401	3.2 [2.3, 4.4]	22 [16, 30]	28 [5.2, 150]	75 [40, 120]	320 [190, 510]	160 [54, 440]
Beam	188	1.4 [1.3, 1.5]	4.4 [4.1, 4.8]	5.7 [1.1, 30]	6.6 [3.7, 9.8]	20 [11, 30]	7.7 [2.4, 23]
Seine	387	0.18 [0.14, 0.22]	0.85 [0.70, 1.0]	1.1 [0.21, 6.0]	3.0 [1.5, 4.4]	9.6 [5.1, 14]	3.7 [1.2, 10]
Dredge	16	0.027 [0.018, 0.035]	0.11 [0.079, 0.15]	0.14 [0.025, 0.74]	1.3 [0.68, 2.1]	4.0 [2.1, 6.4]	1.7 [0.50, 4.8]
Total	1992	4.8 [3.9, 6.0]	27 [21, 35]	80 [26, 260]	87 [51, 130]	360 [220, 540]	190 [84, 470]

resuspension (Fig. 7), which is expected based on the amount of POC that is affected by mixing on an annual basis (13 times more). Nevertheless, the impact of sediment resuspension on mineralization is only 2–3 times lower than that of mixing (Table 3). This non-linearity in the cause-effect relationship is mainly related to the differences in recovery time (hours for the mixing versus days for resuspension). In addition, the results of the ensemble run show that the estimated amount of POC degraded due to MBCF-induced disturbances is, due to the orders-of-magnitude uncertainties in the parameters of the OC model, associated with higher uncertainty than the sediment volume and POC mixing and resuspension estimates (Table 3).

Discussion

Our estimates of MBCF-induced POC mineralization on the NW European shelf amount to $0.27 [0.11, 0.73] \text{ Mt C yr}^{-1}$ (Table 3), which is similar to the $0.4 \pm 1.0 \text{ Mt C yr}^{-1}$ estimated for the North Sea by the 3D biogeochemical modelling study of (Zhang et al. 2024), and two orders of magnitude lower than the NW European shelf estimates of Sala et al. (2021) and Atwood et al. (2024) ($\sim 40 \text{ Mt C yr}^{-1}$; Millage et al. 2025), while using the same 1 G POC mineralization model.

The divergent estimates illustrate that quantifying the impact of MBCF on marine OC sequestration is not a trivial task. Our analysis suggests three main groups of parameters contribute to the overall uncertainty on the impact on marine OC sequestration; (i) spatial distribution of gear-specific MBCF activities, sediment type, POC content, and POC reactivity, (ii) parameters related to estimating the physical impact of MBCF on the seafloor, and (iii) parameterization of the POC mineralization, notably including parameters related to the impact of disturbance on the POC reactivity. Below, we give examples of each group of potential sources of uncertainty, and we put our analysis and the various estimates into perspective, including how the non-normal distribution of some of the parameters can lead to a large increase in the final uncertainty.

The critical first step in any assessment is to know the spatial distribution of MBCF gear activity, sediment type (or silt fraction), POC concentrations, and the reactivity of seafloor POC. Fishing distribution maps were based on VMS-based SAR estimates (ICES 2021) rather than Global Fishing Watch data products derived from Automatic Identification System (AIS). Our study used these estimates, while Sala et al. (2021) and Atwood et al. (2024) started from AIS-derived fisheries distribution, and Zhang et al. (2024) combined AIS and VMS. The VMS-based SAR data have a lower resolution (0.05° by 0.05° , $\sim 20 \text{ km}^2$ in the NW European shelf) than the AIS-based effort distribution maps (0.01° by 0.01° , $\sim 1 \text{ km}^2$, depending on latitude). Our study nevertheless focused on the lower resolution data, because they did not compromise the even lower resolution of the sediment maps (0.125° by 0.125° , Wilson et al. 2018). VMS-based SAR data were preferred over the AIS-derived products, because AIS may not only be turned off, and have limited data coverage (Shepperson et al. 2018) but it may also lead to biased effort estimates (Hintzen et al. 2025) and it is not coupled to logbook data with gear specifications. Detailed logbook data provide a better match of SAR estimates with the categorization of fishing activities into gear groups with diverging seabed impacts. Indeed, VMS-based SAR estimates are based on vessel speeds, but also on métier definitions of gear and targeted species, length overall, and vessel

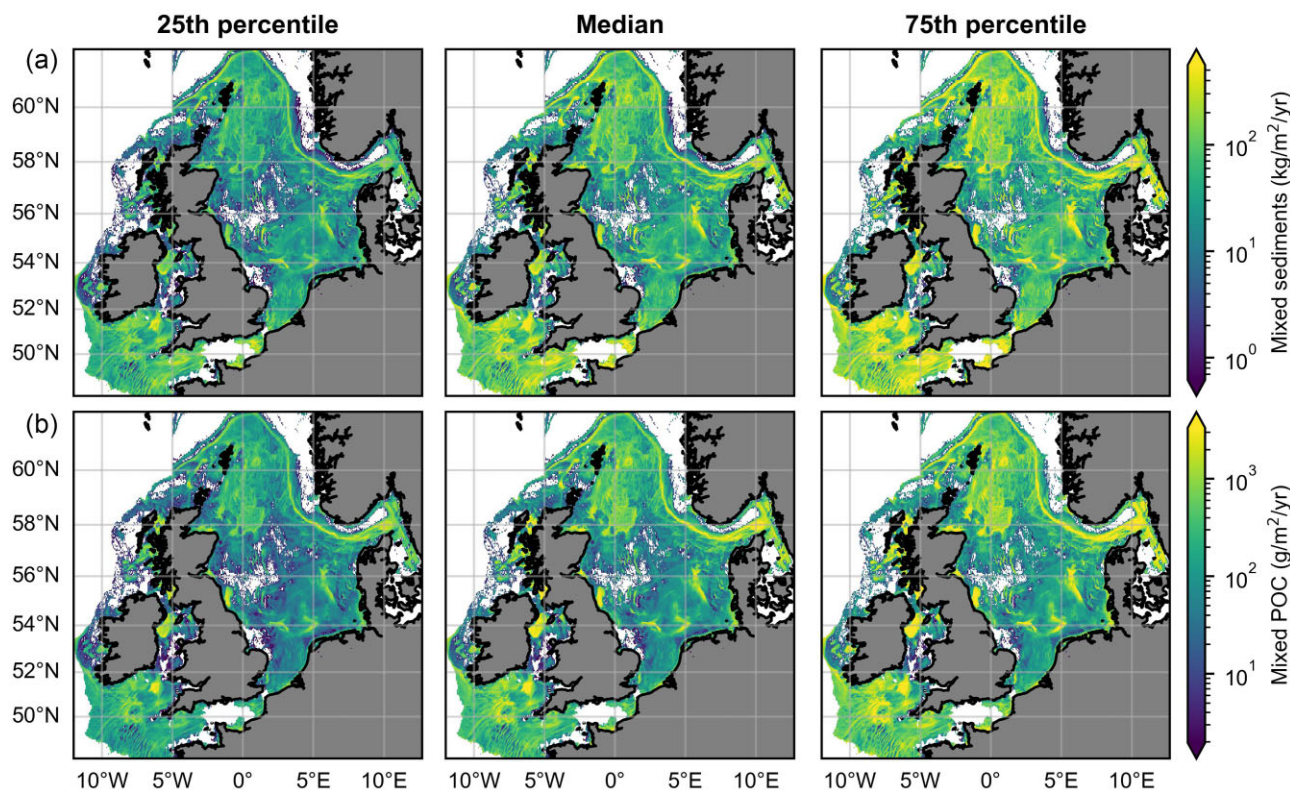


Figure 6. A Sediment mixing and B particulate organic carbon (POC) mixing induced by MBCF fisheries (otter, seine, beam, and dredge) in the NW European shelf for the period 2009–2017, calculated using eqs. (10)–(11) and the POC fraction shown in Fig. 2C. We show the median (left column), 25% percentile (middle column), and 75% percentile (right column) of the Monte Carlo estimate. Spatial maps of individual MBCF gears are shown in Figs. S10–S11.

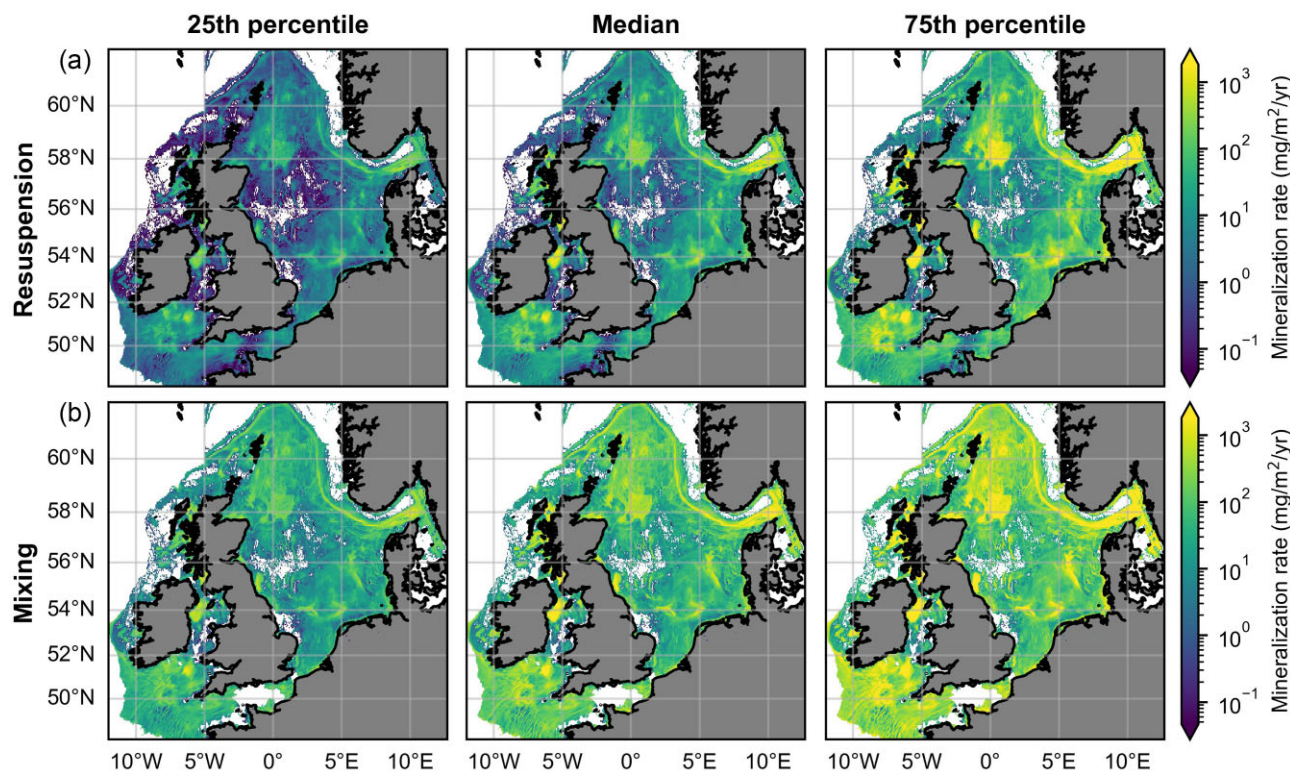


Figure 7. Enhanced organic carbon mineralization due to A sediment resuspension and B sediment mixing induced by MBCF fisheries (otter, seine, beam, and dredge) in the NW European shelf for the period 2009–2017, calculated using eq. (3) and (4). We show the median (left column), 25% percentile (middle column), and 75% percentile (right column) of the Monte Carlo estimate. Spatial maps of individual MBCF gears are shown in Figs. S12–S13.

power, which are specified in the logbook data. These parameters can subsequently be coupled to gear-specific inference of gear width using questionnaire-informed data on métier-tailored gear design, dimensions, and related fishing power (Eigaard et al. 2016, Rijnsdorp et al. 2020). Rickwood et al. (2025) for instance, challenged the reliability of global fishing footprints due to the lack of representative data on commercial gear designs.

The areal extent of our study region was largely defined by the availability of sediment data. In regions such as North America or Northern Europe, detailed spatial maps of silt fraction and POC concentration are available and continuously being improved (see e.g. Wilson et al. 2018, Diesing et al. 2021, Epstein et al. 2024), whereas in other, data-poor, ocean regions these maps are quasi non-existent. Efforts to map the global seabed characteristics could fill that gap but suffer from coarse resolution and the need to extrapolate the data. The larger issue is the lack of any information on the reactivity of the POC in the seabed, which will determine the impact MBCF on the global carbon cycle. Recent efforts to create local spatial maps using qualitative measurements using pyrolysis (such as done in Smeaton and Austin 2022) help, but do not allow for a quantitative estimation of the amount of organic carbon that is mineralized. Recent efforts to constrain organic carbon mineralization rates across several environments show that data coverage is sparse (Freitas et al. 2021) and highlight the need for quantitative measurements of organic carbon reactivity in the seafloor.

To estimate the physical impact, we quantified how much sediment is mixed by the penetration in the seabed and how much sediment is resuspended by the drag that is created by a passing MBCF gear. The penetration depth of the gear is an important parameter to assess the mixing component. A global meta-analysis categorized fishing gears into four generic groups with increasing penetration depths from otter trawls over beam trawls to toothed and hydraulic dredges (Hiddink et al. 2017). The penetration depths of individual gear components vary but have been summarized to an overall gear penetration depth by a weighted average using the spread of the individual gear components over the whole gear width. Métier-specific penetration depths have been inferred using the width of gear components (Rijnsdorp et al. 2020, Szostek et al. 2022), and sediment-specific penetration depths were also inferred from the same global database (Pitcher et al. 2022). While these global meta-analyses are to our knowledge the best available summarizing source on penetration depth, we should be aware that they may be subject to publication bias (e.g. when impacts may be expected hard to quantify, such as for shrimp-targeting beam trawls or Danish seines), or outdated information (e.g. the one study on beam trawl impacts in gravel dates back to 1972). The penetration depth has only been quantified for a limited number of MBCF, leading to a large uncertainty on this parameter (Table 1) and consequent sediment volume estimates (Table 3).

While the uncertainty in the created drag of specific MBCF gears has been accounted for, gear designs are variable and introduce uncertainty, which we could not fully account for. Furthermore, the drag has only been experimentally quantified for a limited number of MBCF gear types and experimental trials. Not all these quantifications included an uncertainty assessment, and a global meta-analysis, as was done for penetration depth, was not available. This lack of empirical data forced us to make assumptions about the drag of, for exam-

ple, seine and dredges, which led to further unaccounted uncertainty. Zhang et al. (2024) also discriminated physical fishing impact from mixing and sediment resuspension. They approached sediment mixing numerically using a scenario-based assessment with two physical mixing coefficients (Porz et al. 2024), while sediment resuspension was based on hydrodynamic drag as in our study. Despite the progress in including sediment resuspension from individual gear components, it should be noted that Rijnsdorp et al. (2021) stressed that the hydrodynamic drag of net panels requires further study to be closer aligned with empirical data. While both studies followed the classification of physical impacts into geotechnical or hydrodynamic effects, as suggested by the review of O'Neill and Ivanovic (2016), Sala et al. (2021) and Atwood et al. (2024) did not discriminate between those physical impacts but focused on the average gear penetration depth only.

Similarly, empirical estimates show that the fishing impacts on OC are uncertain. Epstein et al. (2022) showed no significant effect of mobile fishing in 61% of 49 studies, while 29% reported a decrease and 10% reported an increase in OC. The empirical data underpinning Zhang et al. (2024) illustrated that for a similar mud percentage, there is less OC at higher than at lower MBCF intensities. Tiano *et al.* (2024) concluded that total OC increased in chronically fished areas, though they attributed this to an artefact of MBCF behaviour, where fishing was done more often in productive, and thus POC rich, areas.

Another substantial source of uncertainty is the impact of MBCF disturbances on the reactivity of the POC. To have any impact on POC mineralization, and thus POC sequestration, disturbances must lead to a change in reactivity. There has been very little research directly comparing POC reactivity within the sediment versus in suspension, which leads to a large uncertainty in the potential changes in POC reactivity. This impact of resuspension will also vary between sediment types (see, e.g. Kalapurakkal et al. 2025). Further uncertainty relates to the timescales of impact, as well as potential long-term impacts due to priming (van de Velde et al. 2018, Zhu et al. 2024), or impairment of benthic ecosystems (Katz et al. 2016, Hiddink et al. 2017, Epstein et al. 2022). Our analysis shows that the uncertainty related to the POC mineralization parameters follows a log-normal distribution and is large compared to most other parameters, which leads to almost an order of magnitude increase in the 25%-75% interpercentile range (Table 3). Gains can be made if we can better constrain the POC reactivity parameters through targeted resuspension experiments with different sediment types and depths. Additionally, the differences in reactivity will probably differ locally, as certain systems exhibit higher rates of natural resuspension (such as most transient depositional areas on the NW European shelf; Fig. 1) and will thus be expected to be less affected by anthropogenic disturbance events than systems with lower rates of natural resuspension.

Finally, another major reason for this orders-of-magnitude difference in regional POC mineralization estimates can be sought in the parametrization of the 1 G models. There are essentially 6 parameters that need to be constrained to calculated MBCF-induced POC mineralization using the simple 1 G model (Eq. (3) and (4)); (i) C_{dist} , which is the concentration of disturbed POC, (ii) $t_{recovery}$, which is the duration of the disturbance (i.e. the timescale over which mineralization is calculated); (iii) k , which is the mineralization rate constant. Because we are assessing the impact of a disturbance event, 2

k -values need to be considered; $k_{undisturbed}$, which is the reactivity without any disturbances, and $k_{disturbed}$, which reflects the reactivity change upon disturbance. Like Sala et al. (2021) and Atwood et al. (2024), we derive the parameter C_{dist} from similar gridded POC datasets, which show minimal variation and is thus not expected to be the source of the large discrepancies between studies. Instead, the main difference between our model approaches lies in the parameterization of the first-order rate constant k and the mineralization timescale ($t_{recovery}$).

Hiddink et al. (2023) critically discussed the choice of the first-order decay constant k , suggesting that the use of k values that are too high can inflate the POC mineralization. Atwood et al. (2024) tested a first order of magnitude reduction in decay constant k , and found that this only halved the original model estimates by Sala et al. (2021), and can therefore not fully account for the higher estimates of Sala et al. (2021) and Atwood et al. (2024) versus our study and Zhang et al. (2024). Our study also discriminated between k -values from disturbed versus undisturbed sediments. We chose $k_{undisturbed}$ values (i.e. the POC reactivity in the absence of disturbances) in the range of 10^{-4} – 10^{-1} yr $^{-1}$, which are representative of POC fractions in the first 5–10 cm of continental shelf sediments and agree well with observations from the studied area (Arndt et al. 2013, van de Velde et al. 2018, De Borger et al. 2021, Freitas et al. 2021). We subsequently calculated the impact of MBCF by increasing the $k_{undisturbed}$ values with a factor 1–5, using the estimated impact of oxygen exposure to POC mineralization (Katsev and Crowe 2015), and corrected this MBCF-induced mineralization rate by the mineralization rate under undisturbed conditions (Eq. (3) and (4)). Because the oxic mineralization constants of Katsev and Crowe (2015) were mostly derived from water column data, they integrate all effects of resuspension, including the effect of potential desorption of POC from the mineral matrix (Hedges and Keil 1995, Burdige 2007). This is in contrast to the Sala et al. (2021) approach, which (i) implied that POC in the sediment is unreactive unless it is disturbed by MBCF (i.e. the entire amount of POC disturbed and degraded during an MBCF event contributes to the additional carbon release), and (ii) used k values that are comparatively high and representative of highly reactive POC at the sediment surface, rather than the more unreactive POC within the sediment. Later, Atwood et al. (2024) eased assumption (i) by assuming that 75% of the POC that reaches the sediment is mineralized regardless of whether it has been disturbed by MBCF or not.

Sala et al. (2021), and later Atwood et al. (2024) and Milage et al. (2025), assigned a constant value of 1 year to the recovery timescale (i.e. $t_{recovery} = 1$). Practically, this implies that a passing MBCF gear will impact POC mineralization for one year. More importantly, this treatment also implies that, in the case of more than one MBCF event per year, the impact will count double (for two MBCF events per year), triple (for three MBCF events per year), and so on. Here, we constrain two different $t_{recovery}$ by estimating the time a POC particle remains in suspension (for MBCF-induced resuspension) and the time a POC particle is re-exposed to oxygen mixed into the sediment (for MBCF-induced mixing) (Section 2.3.3). Our estimated impact times are in the order of hours to days. Thus our POC mineralization estimates will be 1.5 (if $t_{recovery}$ is 1 day)–20 (if $t_{recovery}$ is 1 hour) times lower than if using 1 year (note that $t_{recovery}$ is in the exponent in Eq. (2), so changes in $t_{recovery}$ do not linearly scale with changes in the R_{min}).

By estimating the excess mineralization over the natural mineralization that would occur without disturbances, we directly calculate the reduction in POC storage and eventual POC removal through burial. However, our analysis does not account for other carbon cycle feedbacks, such as the impact on primary productivity through nutrient release, the impact of injecting more reactive POC from the surface into deeper, anoxic layers, as well as MBCF impacts on the benthic communities and their effects on remineralization. We additionally are not able to account for altered carbon transport pathways by the MBCF-induced resuspension. Once resuspended, POC could be transported off shelf to the deeper ocean, which would increase the burial—or it could settle on the shelf in a very different environmental context (e.g. more rapidly accumulating sediment, more sandy sediment with higher O₂ supply, etc.) and thus degrade faster/slower than in the undisturbed case where it would remain in its original environmental context. No models currently exist that can account for the full range of environmental conditions and the relation to POC reactivity. Models such as the ones used by (Porz et al. 2024) and (Zhang et al. 2024), have a sediment transport scheme and a very simplified POC mineralization scheme. Their simulations suggest that part of the direct impact of MBCF is offset by secondary impacts, particularly on benthic ecosystem functioning (e.g. fauna mortality), but these assumptions bring in additional uncertainties (e.g. the impact of benthic fauna on POC mineralisation) (Epstein et al. 2022, Tiano et al. 2024a). These 3D models require a lot of work to set up and validate, and include many parameters that introduce additional uncertainties. They also need high computational resources to run and are thus costly and energy intensive. In contrast, simple models like the one employed here allow for a fast first-order estimate of the potential impact, and when employed correctly, give numbers that are close to the more complex models. Our simulation study intends to apply yet another approach to address the same underlying question, i.e. assessment of MBCF effects on carbon sequestration, to contribute to the robustness of the findings (Munafò and Davey Smith 2018), and in case of disparate findings, to stimulate scientific progress by addressing underlying model assumptions. The underlying rationale of our simulation study is not to be found in its direct implementation in management, but rather to contribute to understanding how uncertainties may propagate and require being accounted for prior to making policy actions (Cochrane et al. 2024).

Summary and conclusion

MBCF leaves a major imprint on the sediment dynamics and carbon cycle of continental shelf seas. By re-evaluating the parameterization used in previous high-end model estimates and basing this parametrization on the large body of empirical as well as model derived values, we arrive at a potential increase in NW European shelf OC mineralization of 0.27 [0.11, 0.73] Mt C yr $^{-1}$, which is an order of magnitude smaller the previous estimates but agree well with more recent 3D model estimates. Yet, the estimate presented here still has a considerable uncertainty range of 0.62 Mt C yr $^{-1}$, which is primarily caused by uncertainty in POC reactivity parameters. Uncertainty also arises from unaccounted processes and our generic understanding of sediment mechanics and fishing interactions. Recent efforts to constrain OC mineralization rates across several environments show that data coverage is still sparse (Fre-

itas et al. 2021) and highlight the need for quantitative measurements of OC reactivity in the seafloor. Additionally, the impact of resuspension and mixing on OC mineralization rate is poorly constrained due to the lack of local and mechanistic studies, including experimental studies on impacts of various fishing gears in different sediment types. Targeted studies should aim to experimentally constrain the difference in OC reactivity within the sediment and during resuspension, as well as to better understand gear-specific effects. These experiments will need to be conducted on a wide range of different sedimentary environments.

We have only focused our estimates on the increase of POC mineralization rates following MBCF-induced disturbances. However, in certain transitional systems like the flanks of the Norwegian trench or the Iberian margin, MBCF could potentially accelerate natural transport pathways, potentially leading to more carbon sequestration by bringing POC faster to the deeper parts of the ocean. MBCF can also reduce sedimentary alkalinity production (van de Velde et al. 2025), and increase nutrient release to the water column, which will further influence the carbon cycle. More detailed regional studies that consider regional transport as well as transformations in the water column and seafloor, such as those of Zhang et al. (2024) and Porz et al. (2024), will help to assess the overall impact of MBCF on carbon cycling in the different regional seas, as well as evaluate the efficiency of management plans concerning MBCF fisheries.

Author contributions

Pooran Khedri (Data curation [lead], Formal analysis [equal], Investigation [equal], Writing – original draft [equal]), Olivier Gourgue (Formal analysis [lead], Methodology [supporting], Software [lead], Visualization [equal], Writing – review & editing [supporting]), Jochen Depestele (Conceptualization [equal], Data curation [equal], Formal analysis [supporting], Methodology [supporting], Writing – review & editing [equal]), Sandra Arndt (Conceptualization [supporting], Funding acquisition [equal], Project administration [equal], Writing – review & editing [equal]), and Sebastiaan van de Velde (Conceptualization [lead], Formal analysis [equal], Funding acquisition [equal], Methodology [lead], Project administration [equal], Software [supporting], Supervision [lead], Visualization [equal], Writing – original draft [lead], Writing – review & editing [lead])

Supplementary data

Supplementary data is available at *ICES Journal of Marine Science* online.

Conflict of interest: The authors declare there are no conflict of interest.

Funding

This research is supported by funding from the Belgian Federal Science Policy Office (grant nos FED-tWIN2019-prf-008 and RV/21/DEHEAT to S.A. and S.J.V.). P.K. was supported by a postdoctoral fellowship of the Université Libre de Bruxelles. S.J.V. acknowledges the New Zealand MBIE Strategic Science Investment Fund for support via the NIWA Ocean-Climate Interaction programme.

Data availability

No new data were generated or analysed in support of this research. All model code is available at 10.5281/zenodo.15324607.

References

- Aller RC, Cochran JK. The critical role of bioturbation for particle dynamics, priming potential, and organic C remineralization in marine sediments: local and basin scales. *Front Earth Sci* 2019;7:1–14. <https://doi.org/10.3389/feart.2019.00157>
- Amoroso RO, Pitcher CR, Rijnsdorp AD et al. 2018. Bottom trawl fishing footprints on the world's continental shelves. *Proceedings of the National Academy of Sciences*, 115:E10275–82.
- Arnason TS, Keil RG. Organic–mineral interactions in marine sediments studied using density fractionation and X-ray photoelectron spectroscopy. *Org Geochem* 2001;32:1401–15. [https://doi.org/10.1016/S0146-6380\(01\)00114-0](https://doi.org/10.1016/S0146-6380(01)00114-0)
- Arndt S, Jørgensen BB, LaRowe DE et al. Quantifying the degradation of organic matter in marine sediments: a review and synthesis. *Earth Sci Rev* 2013;123:53–86. Elsevier. <https://doi.org/10.1016/j.earscirev.2013.02.008>
- Atwood TB, Romanou A, DeVries T et al. Atmospheric CO₂ emissions and ocean acidification from bottom-trawling. *Front Earth Sci* 2024;10:1125137. <https://www.frontiersin.org/articles/10.3389/feart.2023.1125137> (Accessed 27 February 2024).
- Berner RA. *Early diagenesis: a theoretical approach*. Princeton, New Jersey, USA: Princeton University Press, 1980:260.
- Berner RA. Burial of Organic Carbon and Pyrite sulfur in the modern ocean: its geochemical and environmental significance. *Am J Sci* 1982;282:451–73. <https://doi.org/10.2475/ajs.282.4.451>
- Bianchi TS. The role of terrestrially derived organic carbon in the coastal ocean: a changing paradigm and the priming effect. *Proc Natl Acad Sci* 2011;108:19473–81. <https://doi.org/10.1073/pnas.1017982108>
- Bockelmann F-D, Puls W, Kleeberg U et al. Mapping mud content and median grain-size of North Sea sediments—A geostatistical approach. *Mar Geol* 2018;397:60–71. <https://doi.org/10.1016/j.margeo.2017.11.003>
- Breimann SA, O'Neill FG, Summerbell K et al. Quantifying the resuspension of nutrients and sediment by demersal trawling. *Cont Shelf Res* 2022;233:104628. <https://doi.org/10.1016/j.csr.2021.104628>
- Burdige DJ. Preservation of Organic Matter in Marine Sediments: controls, Mechanisms, and an Imbalance in Sediment Organic Carbon Budgets? *Chem Rev*, 2007;107:467–85. <https://doi.org/10.1021/cr050347q>
- Canfield DE. Factors influencing organic carbon preservation in marine sediments. *Chem Geol* 1994;114:315–29. [https://doi.org/10.1016/0009-2541\(94\)90061-2](https://doi.org/10.1016/0009-2541(94)90061-2)
- Churchill JH. The effect of commercial trawling on sediment resuspension and transport over the Middle Atlantic Bight continental shelf. *Cont Shelf Res* 1989;9:841–65. [https://doi.org/10.1016/0278-4343\(89\)90016-2](https://doi.org/10.1016/0278-4343(89)90016-2)
- Cochrane KL, Butterworth DS, Hilborn R et al. Errors and bias in marine conservation and fisheries literature: their impact on policies and perceptions. *Mar Policy* 2024;168:106329. <https://doi.org/10.1016/j.marpol.2024.106329>
- De Borger E, Braeckman U, Soetaert K. Rapid organic matter cycling in North Sea sediments. *Cont Shelf Res* 2021;214:104327. <https://doi.org/10.1016/j.csr.2020.104327>
- De Borger E, Tian J, Braeckman U et al. Impact of bottom trawling on sediment biogeochemistry: a modelling approach. *Biogeosciences Discuss* 2020:1–32.
- de Haas H, Boer W, van Weering TCE. Recent sedimentation and organic carbon burial in a shelf sea: the North Sea. *Mar Geol* 1997;144:131–46. [https://doi.org/10.1016/S0025-3227\(97\)00082-0](https://doi.org/10.1016/S0025-3227(97)00082-0)
- Depestele J, Degrendele K, Esmaili M et al. Comparison of mechanical disturbance in soft sediments due to tickler-chain SumWing trawl

- vs. electro-fitted PulseWing trawl. *ICES J Mar Sci* 2019;76:312–29. <https://doi.org/10.1093/icesjms/fsy124>
- Depestele J, Ivanović A, Degrendele K et al. Measuring and assessing the physical impact of beam trawling. *ICES J Mar Sci* 2016;73:i15–26. <https://doi.org/10.1093/icesjms/fsv056>
- Diesing M, Thorsnes T, Bjarnadóttir LR. Organic carbon densities and accumulation rates in surface sediments of the North Sea and Skagerrak. *Biogeosciences* 2021;18:2139–60. <https://doi.org/10.5194/bg-18-2139-2021>
- Durrieu de Madron X, Ferré B, Le Corre G et al. Trawling-induced resuspension and dispersal of muddy sediments and dissolved elements in the Gulf of Lion (NW Mediterranean). *Cont Shelf Res* 2005;25:2387–409. <https://doi.org/10.1016/j.csr.2005.08.002>
- Eigaard O, Bastardie F, Breen M et al. Estimating seabed pressure from demersal trawls, seines, and dredges based on gear design and dimensions. *ICES J Mar Sci* 2016;73:i27–43. <https://doi.org/10.1093/icesjms/fsv099>
- Eigaard O, Bastardie F, Hintzen N et al. The footprint of bottom trawling in European waters: distribution, intensity and seabed integrity. *ICES J Mar Sci* 2017;74:847–65. <https://doi.org/10.1093/icesjms/fsw194>
- Eisma D, Kalf J. Dispersal, concentration and deposition of suspended matter in the North Sea. *J Geol Soc* 1987;144:161–78. <https://doi.org/10.1144/gsjgs.144.1.0161>
- Emeis K-C, van Beusekom J, Callies U et al. The North Sea—A shelf sea in the Anthropocene. *J Mar Syst* 2015;141:18–33. <https://doi.org/10.1016/j.jmarsys.2014.03.012>
- Epstein G, Fuller SD, Hingmire D et al. Predictive mapping of organic carbon stocks in surficial sediments of the Canadian continental margin. *Earth Syst Sci Data* 2024;16:2165–95. <https://doi.org/10.5194/essd-16-2165-2024>
- Epstein G, Middelburg JJ, Hawkins JP et al. The impact of mobile demersal fishing on carbon storage in seabed sediments. *Global Change Biol* 2022;28:2875–94. <https://doi.org/10.1111/gcb.16105>
- Freitas FS, Pika PA, Kasten S et al. New insights into large-scale trends of apparent organic matter reactivity in marine sediments and patterns of benthic carbon transformation. *Biogeosciences* 2021;18:4651–79. <https://doi.org/10.5194/bg-18-4651-2021>
- Glud RN. Oxygen dynamics of marine sediments. *Mar Biol Res* 2008;4:243–89. <https://doi.org/10.1080/17451000801888726>
- Halpern BS, Frazier M, Afflerbach J et al. Recent pace of change in human impact on the world's ocean. *Sci Rep* 2019;9:11609. <https://doi.org/10.1038/s41598-019-47201-9>
- Halpern BS, Walbridge S, Selkoe KA et al. A global map of human impact on marine ecosystems. *Science* 2008;319:948–52. <https://doi.org/10.1126/science.1149345>
- Hartnett HE, Keil RG, Hedges JI et al. Influence of oxygen exposure time on organic carbon preservation in continental margin sediments. *Nature* 1998;391:572–5. <https://doi.org/10.1038/35351>
- Hedges JI, Keil RG. Sedimentary organic matter preservation: an assessment and speculative synthesis. *Mar Chem* 1995;49:81–115. [https://doi.org/10.1016/0304-4203\(95\)00008-F](https://doi.org/10.1016/0304-4203(95)00008-F)
- Hiddink JG, Jennings S, Sciberras M et al. 2017 Global analysis of depletion and recovery of seabed biota after bottom trawling disturbance. *Proceedings of the National Academy of Sciences of the United States of America*, 114:8301–6. National Academy of Sciences.
- Hiddink JG, Van De Velde SJ, McConnaughey RA et al. Quantifying the carbon benefits of ending bottom trawling. *Nature* 2023;617:E1–2. <https://doi.org/10.1038/s41586-023-06014-7>
- Hintzen NT, Brigden K, Kaastra H-J et al. Bias in Global Fishing Watch AIS data analyses results in overestimate of Northeast Atlantic pelagic fishing impact. *ICES J Mar Sci* 2025;82:fsaf033. <https://doi.org/10.1093/icesjms/fsaf033>
- ICES. 2021 OSPAR request on the production of spatial data layers of fishing intensity/pressure. report. ICES Advice: Special Requests. https://ices-library.figshare.com/articles/report/OSPAR_request_on_the_production_of_spatial_data_layers_of_fishing_intensity_pressure/18639182/1 (Accessed 12 October 2023).
- ICES. 2022 Greater North Sea ecoregion—fisheries overview. report. ICES Advice: Fisheries Overviews. https://ices-library.figshare.com/articles/report/Greater_North_Sea_ecoregion_fisheries_overview/21641360/1 (Accessed 10 February 2024).
- ICES. EU request on spatial trade-off analysis between reducing the extent of mobile bottom-contacting gear (MBCG) disturbance to seabed habitats and potential costs to fisheries. report. ICES Advice: Special Requests. 2024. https://ices-library.figshare.com/articles/report/EU_request_on_spatial_trade-off_analysis_between_reducing_the_extent_of_mobile_bottom-contacting_gear_MBCG_disturbance_to_seabed_habitats_and_potential_costs_to_fisheries/25601121/1 (Accessed 6 June 2024).
- Kaiser MJ, Hiddink JG. Food subsidies from fisheries to continental shelf benthic scavengers. *Mar Ecol Prog Ser* 2007;350:267–76. <https://doi.org/10.3354/meps07194>
- Kalapurakkal HT, Dale AW, Schmidt M et al. Sediment resuspension in muddy sediments enhances pyrite oxidation and carbon dioxide emissions in Kiel Bight. *Commun Earth Environ* 2025a;6:1–14.
- Kalapurakkal HT, Dale AW, Schmidt M et al. Sediment resuspension in muddy sediments enhances pyrite oxidation and carbon dioxide emissions in Kiel Bight. *Commun Earth Environ* 2025b;6:1–14.
- Katsev S, Crowe SA. Organic carbon burial efficiencies in sediments: the power law of mineralization revisited. *Geology* 2015;43:607–10. <https://doi.org/10.1130/G36626.1>
- Katz T, Yahel G, Tunnicliffe V et al. The silica cycle in a Northeast Pacific fjord; the role of biological resuspension. *Prog Oceanogr* 2016;147:10–21. <https://doi.org/10.1016/j.pocean.2016.07.004>
- Keil R. Anthropogenic forcing of carbonate and organic carbon preservation in marine sediments. *Ann Rev Mar Sci* 2017;9:151–72. <https://doi.org/10.1146/annurev-marine-010816-060724>
- LaRowe DE, Arndt S, Bradley JA et al. The fate of organic carbon in marine sediments—New insights from recent data and analysis. *Earth Sci Rev* 2020;204:103146. <https://doi.org/10.1016/j.earscirev.2020.103146>
- LaRowe DE, Van Cappellen P. Degradation of natural organic matter: a thermodynamic analysis. *Geochim Cosmochim Acta* 2011;75:2030–42. <https://doi.org/10.1016/j.gca.2011.01.020>
- Lee TR, Wood WT, Phrampus BJ. A machine learning (kNN) approach to predicting global seafloor total organic carbon. *Global Biogeochem Cycles* 2019;33:37–46. <https://doi.org/10.1029/2018GB005992>
- Legge O, Johnson M, Hicks N et al. Carbon on the Northwest European Shelf: contemporary budget and future influences. *Front Mar Sci*. 2020, 7, 143. <https://doi.org/10.3389/fmars.2020.00143>
- Matear L, Vina-Herbon C, Woodcock KA. et al. Extent of physical disturbance to benthic habitats: fisheries with mobile bottom-contacting gears. OSPAR, 2023: *The 2023 Quality Status Report for the Northeast Atlantic*. London: OSPAR Commission, 2023. <https://oap.ospar.org/en/ospar-assessments/quality-status-reports/qsr-2023/indicator-assessments/phys-dist-habs-fisheries/> (Accessed 6 June 2024).
- Mayer LM. Surface area control of organic carbon accumulation in continental shelf sediments. *Geochim Cosmochim Acta* 1994;58:1271–84. [https://doi.org/10.1016/0016-7037\(94\)90381-6](https://doi.org/10.1016/0016-7037(94)90381-6)
- McCandliss RR, Jones SE, Hearn M et al. Dynamics of suspended particles in coastal waters (southern North Sea) during a spring bloom. *J Sea Res* 2002;47:285–302. [https://doi.org/10.1016/S1385-1101\(02\)00123-5](https://doi.org/10.1016/S1385-1101(02)00123-5)
- Middelburg JJ, Levin LA. Coastal hypoxia and sediment biogeochemistry. *Biogeosciences*, 2009;6:1273–93. <https://doi.org/10.5194/bg-6-1273-2009>
- Middelburg JJ, Soetaert K, Herman PMJ. Empirical relationships for use in global diagenetic models. *Deep Sea Res Part I* 1997;44:327–44. Pergamon. [https://doi.org/10.1016/S0967-0637\(96\)00101-X](https://doi.org/10.1016/S0967-0637(96)00101-X)

- Millage KD, Mayorga J, Orofino S *et al.* The value of bottom trawling in Europe. *Research Square* 2025. <https://www.researchsquare.com/article/rs-6298588/v1> (Accessed 11 April 2025).
- Munafò MR, Smith D, 2018 Robust research needs many lines of evidence. *Nature* 553:399–401. <https://doi.org/10.1038/d41586-018-01023-3>
- Noack T, Frandsen RP, Krag LA *et al.* Codend selectivity in a commercial Danish anchor seine. *Fish Res* 2017;186:283–91. <https://doi.org/10.1016/j.fishres.2016.10.006>
- O'Neill FG, Ivanovic A. The physical impact of towed demersal fishing gears on soft sediments. *ICES J Mar Sci* 2016;73:i5–i14.
- O'Neill FG, Noack T. The geometry and dynamics of Danish anchor seine ropes on the seabed. *ICES J Mar Sci* 2021;78:125–33.
- O'Neill FG, Robertson M, Summerbell K *et al.* The mobilisation of sediment and benthic infauna by scallop dredges. *Mar Environ Res* 2013;90:104–12.
- O'Neill FG, Summerbell K. The mobilisation of sediment by demersal otter trawls. *Mar Pollut Bull* 2011;62:1088–97.
- O'Neill FG, Summerbell KD. The hydrodynamic drag and the mobilisation of sediment into the water column of towed fishing gear components. *J Mar Syst* 2016;164:76–84.
- Palder OJ, Feekings JP, Fraser S *et al.* Approaching single-species exclusion in mixed demersal trawl fisheries. *Ocean Coast Manag* 2023;242:106672.
- Paradis S, Pusceddu A, Masqué P *et al.* Organic matter contents and degradation in a highly trawled area during fresh particle inputs (Gulf of Castellammare, southwestern Mediterranean). *Biogeosciences* 2019;16:4307–20. <https://doi.org/10.5194/bg-16-4307-2019>
- Pilskaln CH, Churchill JH, Mayer LM. Resuspension of sediment by bottom trawling in the Gulf of Maine and potential geochemical consequences. *Conserv Biol* 1998;12:1223–9. <https://doi.org/10.1046/j.1523-1739.1998.0120061223.x>
- Pitcher CR, Hiddink JG, Jennings S *et al.* Trawl impacts on the relative status of biotic communities of seabed sedimentary habitats in 24 regions worldwide. *Proc Natl Acad Sci* 2022;119:e2109449119. Proceedings of the National Academy of Sciences. <https://doi.org/10.1073/pnas.2109449119>
- Polet H, Fonteyne R. Huidige vistuigen en visserijmethodes in de Belgische Zeevisserij. *Mededelingen van het Rijksstation voor Zeevisserij (Belgium)*. no. 237. 1995. <https://agris.fao.org/search/en/providers/123819/records/6473594053aa8c8963079bee> (Accessed 4 April 2025).
- Porz L, Zhang W, Christiansen N *et al.* Quantification and mitigation of bottom-trawling impacts on sedimentary organic carbon stocks in the North Sea. *Biogeosciences* 2024;21:2547–70. <https://doi.org/10.5194/bg-21-2547-2024>
- Prado J. *Fisherman's workbook*. Oxford, UK: Fishing News Books, 1990, 185.
- Precht E, Franke U, Polerecky L *et al.* Oxygen dynamics in permeable sediments with wave-driven pore water exchange. *Limnol Oceanogr* 2004;49:693–705. <https://doi.org/10.4319/lo.2004.49.3.0693>
- Reid AJ. A net drag formula for pelagic nets. *Scott Fish Res Rep* 1977;7:12.
- Ricker M, Stanev EV. Circulation of the European northwest shelf: a lagrangian perspective. *Ocean Sci* 2020;16:637–55. <https://doi.org/10.5194/os-16-637-2020>
- Rickwood M, Kerry C, Eigaard OR *et al.* Regional variation in active bottom-contacting gear footprints. *Fish Fish* 2025;26:488–503. <https://doi.org/10.1111/faf.12893>
- Rijnsdorp AD, Depestele J, Molenaar P *et al.* Sediment mobilization by bottom trawls: a model approach applied to the Dutch North Sea beam trawl fishery. *ICES J Mar Sci* 2021;78:1574–86. <https://doi.org/10.1093/icesjms/fsab029>
- Rijnsdorp AD, Hiddink JG, van Denderen PD *et al.* Different bottom trawl fisheries have a differential impact on the status of the North Sea seafloor habitats. *ICES J Mar Sci* 2020;77:1772–86. <https://doi.org/10.1093/icesjms/fsaa050>
- Rooze J, Zeller MA, Gogina M *et al.* Bottom-trawling signals lost in sediment: a combined biogeochemical and modeling approach to early diagenesis in a perturbed coastal area of the southern Baltic Sea. *Sci Total Environ* 2024;906:167551. <https://doi.org/10.1016/j.scitotenv.2023.167551>
- Sala E, Mayorga J, Bradley D *et al.* Protecting the global ocean for biodiversity, food and climate. *Nature* 2021;592:397–402. <https://doi.org/10.1038/s41586-021-03371-z>
- Shepperson JL, Hintzen NT, Szostek CL *et al.* A comparison of VMS and AIS data: the effect of data coverage and vessel position recording frequency on estimates of fishing footprints. *ICES J Mar Sci* 2018;75:988–98. <https://doi.org/10.1093/icesjms/fsx230>
- Smeaton C, Austin WEN. Quality not quantity: prioritizing the management of sedimentary organic matter across continental shelf seas. *Geophys Res Lett* 2022;49:e2021GL097481. <https://doi.org/10.1029/2021GL097481>
- Soetaert K, Herman PMJ, Middelburg JJ. A model of early diagenetic processes from the shelf To abyssal depths. *Geochim Cosmochim Acta* 1996;60:1019–40. [https://doi.org/10.1016/0016-7037\(96\)00013-0](https://doi.org/10.1016/0016-7037(96)00013-0)
- Steinacher M, Joos F, Frölicher TL *et al.* Projected 21st century decrease in marine productivity: a multi-model analysis. *Biogeosciences* 2010;7:979–1005. <https://doi.org/10.5194/bg-7-979-2010>
- Sutherland WJ, Bennett C, Brotherton PNM. *et al.* A horizon scan of global biological conservation issues for 2024. *Trends Ecol Evol* 2024;39:89–100.
- Szostek CL, Hiddink JG, Sciberras M *et al.* A tool to estimate the contribution of fishing gear modifications to reduce benthic impact. *J Ind Ecol* 2022;26:1858–70. <https://doi.org/10.1111/jiec.13366>
- Tiano J, De Borger E, Paradis S *et al.* Global meta-analysis of demersal fishing impacts on organic carbon and associated biogeochemistry. *Fish and Fisheries* 2024;25:936–50. <https://doi.org/10.1111/faf.12855>
- Tiano J, Witbaard R, Gerkema T *et al.* Biogeochemical dynamics in a marine storm demonstrates differences between natural and anthropogenic impacts. *Sci Rep* 2024b;14:8802. <https://doi.org/10.1038/s41598-024-59317-8>
- Tiano JC, Witbaard R, Bergman MJN *et al.* Acute impacts of bottom trawl gears on benthic metabolism and nutrient cycling. *ICES J Mar Sci* 2019;76:1917–30. <https://doi.org/10.1093/icesjms/fsz060>
- Turrell WR. New hypotheses concerning the circulation of the northern North Sea and its relation to North Sea fish stock recruitment. *ICES J Mar Sci* 1992;49:107–23. <https://doi.org/10.1093/icesjms/49.1.107>
- Vanderklift MA, Herr D, Lovelock CE. *et al.* A guide to international climate mitigation policy and finance frameworks relevant to the protection and restoration of blue carbon ecosystems. *Frontiers in Marine Science* 2022;9:872064. <https://www.frontiersin.org/articles/10.3389/fmars.2022.872064> (Accessed 6 June 2024).
- van de Velde SJ, Hidalgo-Martinez S, Callebaut I *et al.* Burrowing fauna mediate alternative stable states in the redox cycling of salt marsh sediments. *Geochim Cosmochim Acta* 2020;276:31–49. <https://doi.org/10.1016/j.gca.2020.02.021>
- van de Velde SJ, Hylén A, Meysman FJR. Ocean alkalinity destruction by anthropogenic seafloor disturbances generates a hidden CO₂ emission. *Sci Adv* 2025;11:eadp9112. <https://doi.org/10.1126/sciadv.adp9112>
- van de Velde SJ, Van Lancker V, Hidalgo-Martinez S *et al.* Anthropogenic disturbance keeps the coastal seafloor biogeochemistry in a transient state. *Sci Rep* 2018;8:1–10. <https://doi.org/10.1038/s41598-018-23925-y>
- van Nugteren P, Moodley L, Brummer GJ *et al.* Seafloor ecosystem functioning: the importance of organic matter priming. *Mar Biol* 2009;156:2277–87. <https://doi.org/10.1007/s00227-009-1255-5>
- Wilson RJ, Speirs DC, Sabatino A *et al.* A synthetic map of the north-west European Shelf sedimentary environment for applications in marine science. *Earth System Science Data* 2018;10:109–30. <https://doi.org/10.5194/essd-10-109-2018>

- Zhang W, Porz L, Yilmaz R *et al.* Long-term carbon storage in shelf sea sediments reduced by intensive bottom trawling. *Nat Geosci* 2024;17:1268–76. <https://doi.org/10.1038/s41561-024-01581-4>
- Zhu Q-Z, Yin X, Taubner H *et al.* Secondary production and priming reshape the organic matter composition in marine sediments.

Sci Adv 2024;10:eadm8096. <https://doi.org/10.1126/sciadv.adm8096>

Handling editor: Saša Raicevich